HHS Public Access

Author manuscript

Biomaterials. Author manuscript; available in PMC 2016 June 26.

Published in final edited form as:

Biomaterials. 2015 August ; 60: 82–91. doi:10.1016/j.biomaterials.2015.03.055.

Physiologic force-frequency in engineered heart muscle by electromechanical stimulation

Amandine F. G. Godier-Furnémont, PhD[1,2,4,*], **Malte Tiburcy, MD**[1,4,*], **Eva Wagner, PhD**[3,4], **Matthias Dewenter, MD**[1,4], **Simon Lämmle, PhD**[1,4], **Ali El-Armouche, MD**[1,4], **Stephan E. Lehnart, MD**[3,4], **Gordana Vunjak-Novakovic, PhD**[2], and **Wolfram-Hubertus Zimmermann, MD**[1,4]

[1]Institute of Pharmacology, Heart Research Center Göttingen, University Medical Center Göttingen, Georg-August-University Göttingen, Germany 37075

[2]Department of Biomedical Engineering, Columbia University, New York, NY 10032

[3]Clinic of Cardiology and Pulmonology, Heart Research Center Göttingen, University Medical Center Göttingen, Georg-August-University Göttingen, Germany 37075

[4]German Center for Cardiovascular Research (DZHK), partner site Göttingen, Germany 37075

Abstract

A hallmark of mature mammalian ventricular myocardium is a positive force-frequency relationship (FFR). Despite evidence of organotypic structural and molecular maturation, a positive FFR has not been observed in mammalian tissue engineered heart muscle. We hypothesized that concurrent mechanical and electrical stimulation at frequencies matching physiological heart rate will result in functional maturation. To this end, we investigated the role of such biomimetic mechanical and electrical stimulation in functional maturation in engineered heart muscle (EHM) comprising collagen type I and neonatal rat heart cells. Following tissue consolidation (8 days), EHM were subjected to electrical field stimulation at 0, 2, 4, or 6 Hz for 5 days, while strained on flexible poles to facilitate auxotonic contractions. EHM stimulated at 2 and 4 Hz displayed a similarly enhanced inotropic reserve, but a clearly diverging FFR. The positive FFR in 4 Hz stimulated EHM was associated with reduced calcium sensitivity, frequency-dependent acceleration of relaxation, and enhanced post-rest potentiation. This was paralleled on the cellular level with improved calcium storage and release capacity of the sarcoplasmic reticulum, increased amounts of SERCA2a and RyR2 protein, and enhanced T-tubulation. We demonstrate that electromechanical stimulation at a frequency matching closely the physiological heart rate supports functional maturation in mammalian EHM. The observed positive FFR in EHM has important implications for the applicability of EHM in cardiovascular research and drug testing.

[*]AGF and MT have contributed equally to this study

Disclosures

The authors have declared that no conflict of interest exists.

Keywords

Heart; Tissue engineering; Myocardium; Biophysical properties; Force of contraction; Force frequency relationship; Calcium handling; T-tubulation; Maturation

1. Introduction

Mature mammalian ventricular myocardium exhibits a positive force-preload relationship (Frank-Starling mechanism) and a positive force–frequency relationship (FFR; Bowditch phenomenon), both of which are of critical importance for the contractile performance of healthy myocardium (1). Loss of both mechanisms along with fundamental alterations in excitation-contraction coupling are key features in heart failure (2, 3). The positive FFR seems to be intrinsically dependent on the maturity of the intracellular calcium stores, the sarcoplasmic reticulum (SR), and T-tubulation, which develop postnatally, allowing for rapid intracellular recycling of calcium during systole and diastole (4–6).

Tissue engineering aims at recapitulating myocardial physiology and pathology *in vitro* (7). Over the past two decades, morphological (e.g., tissue anisotropy), molecular (e.g., low expression of fetal genes), and functional data (e.g., positive Frank-Starling mechanism) have provided compelling evidence in support of the notion that tissue engineered myocardium is more mature than classical two-dimensional cultures (8, 9). Mechanical (10, 11) and electrical (12, 13) stimulation were associated with enhanced maturation. Dynamic mechanical stimulation (DMS) designed to facilitate auxotonic contractions against a defined resilient load was most effective in enhancing maturation in engineered heart muscle (EHM) (14, 15). Similarly, optimization of electrical field stimulation improved contractile parameters (12, 13, 16, 17) and enhanced hypertrophic growth (18). Although intuitively of great interest, experiments combining these paradigms in a physiology-adapted manner have not been reported,. Similarly, no studies to date have enabled the generation of tissue engineered myocardium with a mature, i.e., positive FFR, which is a classical hallmark of mammalian ventricular myocardium (1, 8). Importantly, the positive FFR is critical for the *in vitro* screening and validation of chronotropic and inotropic drugs.

Because heart muscle development and maturation depend on electro-mechanical inputs, we anticipated that supporting auxotonically contracting, i.e., mechanically loaded, EHM by electrical stimulation at frequencies observed in neonatal heart (~4–8 Hz in 1–14 day old rats (19)) would enhance functional maturation and recapitulate postnatal development with SR-functionality and T-tubulation. We therefore investigated the role of mechanistic underpinning of the continuous electro-mechanical “training” at physiological frequencies (4 Hz) in functional maturation in tissue-engineered myocardium. Using this approach, we achieved for the first time a positive FFR in mammalian tissue engineered myocardium. This result provides a compelling argument for the use of electro-mechanical stimulation regimens as a means to achieve a fundamental physiologic property necessary for the utilization of EHM for *in vitro* studies into cardiovascular physiology and pharmacology.

2. Results

2.1 Electro-Mechanical Stimulation Matures Contractile Function of EHM

EHMs were cultured under DMS (Figure 1) applied after a consolidation phase to support auxotonic contractions (14). On culture day 8, spontaneous beating frequency of EHM was 1.23 ± 0.15 Hz (n=50). Within 48 hours, EHMs could be reproducibly captured at 2 and 4 Hz, but not at 6 Hz. After 5 days of electro-mechanical stimulation (culture day 13), we observed a marked drop in spontaneous beating frequency – an indicator of maturation, that was most pronounced in the 4 Hz group (Unstimulated: 0.63 ± 0.11 Hz [n=17]; 2 Hz group: 0.45 ± 0.15 Hz [n=16]; 4 Hz group: 0.35 ± 0.15 Hz [n=17]). Electrical stimulation increased force of contraction (FOC) of EHMs at maximum extracellular calcium (2.8 mmol/L) compared to mechanically stimulated EHM (Unstimulated: 0.65 ± 0.08 mN [n=16]; 2 Hz: 0.95 ± 0.11 mN [n=11]; 4 Hz: 1.2 ± 0.08 mN [n=16]; Figure 2A). Notably, a significant shift in the calcium sensitivity was observed in the 4 Hz group (EC_{50} for calcium: 0.45 ± 0.02 mmol/L [Unstim]; 0.45 ± 0.03 mmol/L [2 Hz]; 0.74 ± 0.06 mmol/L [4 Hz]), suggesting maturation of the calcium handling machinery. Importantly, electrical stimulation did not influence total cell number (combined average from 22 EHMs: 6.1 ± 0.3 × 10^5; Figure S1A), cell viability after enzymatic dispersion of EHM (combined average from 22 EHMs: 45 ± 2%; Figure S1B), cardiomyocyte number (combined average from 22 EHMs: 0.75 ± 0.07 × 10^5; Figure S1C), and cardiomyocyte size assessed by cytometry for actinin fluorescence signal intensity per cell (average from 8–10 EHM per group; Figure S1D). The latter data were confirmed by morphometric quantification of the cardiomyocyte area (Unstimulated: 548 ± 62 μm^2 [n=11 cardiomyocytes]; 2 Hz: 564 ± 46 μm^2 [n=9 cardiomyocytes]; 4 Hz: 560 ± 38 μm^2 [n=17 cardiomyocytes]; Figure S1D). Cardiomyocytes from postnatal day-13 were larger (931 ± 61 μm^2; n=20 cardiomyocytes) in comparison to any of the investigated EHM groups ($P < 0.05$ by ANOVA with Bonferroni multiple comparison test).

2.2 Positive Force-Frequency Relationship in 4 Hz stimulated EHM

A classical property of mature non-failing ventricular myocardium is a positive FFR, associated typically with frequency-dependent acceleration of relaxation (FDAR) (1). Neither a positive FFR nor FDAR have been reported in any mammalian model of tissue engineered myocardium (8). In EHM developed under electro-mechanical stimulation at 4 Hz – a physiological heart rate in 1 day old rats (19, 20) - we now find for the first time a clearly positive FFR (Figure 2B–C), demonstrating that electrical stimulation at physiological frequency is critical for functional maturation. Consistently, we observed in the 4 Hz EHM a markedly shortened relaxation time and enhanced FDAR (Figure 2D).

2.3 Electro-Mechanical Stimulation Matures Calcium Handling in EHMs

Cardiomyocytes isolated from either 13-day old rats or day 13 EHMs were loaded with fura-2 dye followed by calcium transient imaging at 1 Hz stimulation. Cardiomyocytes from the 4 Hz EHM group exhibited calcium transients closely resembling those derived from 13-day old rat myocardium (representative traces, Figure 3A). In contrast, both unstimulated and 2 Hz EHM-derived cardiomyocytes displayed comparatively delayed time-to-peak (Unstimulated: 64 ± 6 ms [n=10 cardiomyocytes]; 2 Hz: 61 ± 5 ms [n=10 cardiomyocytes];

4 Hz: 53 ± 3 ms [n=11 cardiomyocytes]; 13-day heart-derived cardiomyocytes: 35 ± 2 ms [n=7]) and prolonged relaxation times (time-to-baseline, Unstim: 391 ± 46 ms [n=6 cardiomyocytes]; 2 Hz: 393 ± 34 s [n=7 cardiomyocytes]; 4 Hz: 293 ± 24 ms [n=6 cardiomyocytes]; 13-day heart-derived cardiomyocytes: 205 ± 9 ms [n=7]), consistent with the relaxation differences seen on the tissue level (Figure 2D).

2.4 Functional Evidence for Increased SR Calcium Storage and Release

EHMs subjected to isometric force measurements at day 13 were subsequently tested for post-rest-potentiation (PRP) to assess SR calcium storage capacity (21⁻23). Following stimulation pauses of 10, 20, and 30 seconds, post-rest twitches showed maximal potentiation (combined average from 48 EHM: +21 ± 1%) in the 4 Hz EHM group; Unstimulated (combined average from 48 EHM: +15 ± 1%) and 2 Hz EHM (combined average from 33 EHM: +16 ± 1%; Figure 3B). Increased SR storage and release capacity were further supported by calcium imaging in quiescent EHM-derived cardiomyocytes, subjected to caffeine puffs (10 mmol/L) for SR calcium depletion (Figure 3C). The caffeine induced calcium release provided evidence for increased SR storage capacity in cardiomyocytes from EHMs stimulated at 2 and 4 Hz (calcium transient peak height [$\Delta F/F_0$], Unstimulated: 0.54 ± 0.06 [n=6 cardiomyocytes]; 2 Hz: 0.77 ± 0.07 [n=6]; 4 Hz: 0.76 ± 0.07 [n=6]), being in line with the similarly enhanced maximal inotropic capacity in 2 Hz and 4 Hz stimulated EHMs (Figure 2A). There was a trend for faster caffeine-induced calcium release (time-to-peak [90%], Unstimulated: 245 ± 25 ms [n=6]; 2 Hz: 239 ± 41 ms [n=6]; 4 Hz: 173 ± 27 ms [n=6 cardiomyocytes] – $P = 0.08$ Unstimulated vs. 4 Hz) and a significant acceleration of calcium decay in 4 Hz EHM (Unstimulated: 537 ± 64 ms [n=9]; 2 Hz: 380 ± 67 ms [n=9]; 4 Hz: 301 ± 40 ms [n=10]), suggesting enhanced function of the SR calcium release channel (RyR2) and the sarco/endoplasmic reticulum Ca^{2+}-ATPase (SERCA2a).

2.5 Electro-Mechanical Stimulation Enhanced SR Calcium Release via RyR2

The increased SR function with faster calcium release (Figures 3) pointed towards an improved RyR function. To further investigate this phenomenon, we treated day-13 EHMs with ryanodine (1 μmol/L) to block calcium-mediated calcium release. Ryanodine elicited the anticipated negative inotropic effect in all groups, with a most pronounced effect in 4 Hz EHM (Unstimulated: −12 ± 2% [n=8]; 2 Hz: −13 ± 2% [n=8]; 4 Hz: −25 ± 5% [n=8]; Figure 4A–B). In line with its mechanism of action, ryanodine similarly slowed contraction time in all groups (Figure 4C). Immunofluorescent staining of RyR2 confirmed regular organization in striations, particularly at the Z-band co-stained with α-actinin (Figure 4D). There were no obvious differences in RyR2 localization in the unstimulated and electrically stimulated EHM groups. Western blotting revealed a 2-fold increase of RyR2 protein, which was not statistically significant (Unstimulated: 1.0 ± 0.1 [n=8]; 2 Hz: 1.2 ± 0.1 [n=8]; 4 Hz: 2.3 ± 0.7 [n=8]; $P = 0.07$; Figure 4E). LTCC protein abundance was similar in all investigated groups (Figure 4F).

2.6 Electro-Mechanical Stimulation Enhanced SERCA2a Mediated SR Calcium Reuptake

Maturation of calcium handling in cardiomyocytes involves SR calcium storage. Calcium reuptake in diastole into the SR is mediated via SERCA2a; inside the SR, calcium is

sequestered by CSQ2. In line with an enhanced SR calcium re-uptake (Figures 3), we observed higher SERCA2a protein in 4 Hz EHM (1.6 ± 0.2 fold; $P < 0.05$ vs. Unstimulated) with similar CSQ2 abundance in all groups (Figure 5A). Pharmacological inhibition of SERCA2a with thapsigargin (1 μmol/L) induced the anticipated reduction in SR calcium reuptake in EHM-derived cardiomyocytes (Figure 5B; Unstimulated: −24 ± 6% [n=6], 2 Hz: −39 ± 12% [n=7], and 4 Hz: −52 ± 13% [n=6]).

2.7 Enhanced T-tubulation under Electro-Mechanical Stimulation

Although RyR2 and by extension the junctional SR (jSR) may be localized properly at the Z-band level as evidenced by immunofluorescence microscopy, its localization does not prove T-tubule formation by *bona fide* sarcolemmal membrane invagination and juxtaposition with the jSR. To assess whether T-tubules developed as continuous intracellular membrane extensions of the sarcolemma, we applied wheat germ agglutinin (WGA) to cardiomyocytes isolated from 13 day old EHM. Quantification of the WGA signal intensity by flow cytometry in α-actinin positive cardiomyocytes was used to estimate the extent of T-tubulation. EHMs stimulated at 4 Hz exhibited the largest surface membrane relative to the unstimulated EHMs (Unstimulated: 1 ± 0.01 [cardiomyocytes from 10 EHM]; 2 Hz: 1.1 ± 0.1 fold [cardiomyocytes from 8 EHM]; 4 Hz: 1.3 ± 0.1 fold [cardiomyocytes from 9 EHM]; Figure 6A). There was no difference in cardiomyocyte size between the investigated groups (Figure S1D), supporting the notion that T-tubulation was enhanced. We next labeled EHM-derived cardiomyocytes with a direct live cell membrane dye, di-8-ANEPPS, to scrutinize these findings and assess the specific morphology of the T-tubular membrane network (Figure 6B+C). These data confirmed enhanced T-tubulation at 4 Hz and further demonstrated a mainly longitudinal T-tubule orientation in cardiomyocytes within EHMs, independent of the electro-mechanical stimulation regime (Figure 6D). In contrast, day-13 neonatal rat cardiomyocytes showed ~25% of T-tubular components being oriented perpendicularly to the main cell axis.

3. Discussion

Key biophysical properties of mature and healthy myocardium are: (i) a positive force-preload relationship (*aka* Frank-Starling mechanism) and (ii) a positive FFR (*aka* Bowditch phenomenon) (1–3). The Frank-Starling mechanism has been recapitulated in several models of tissue engineered myocardium, suggesting some physiological development (8). The lack of a positive FFR in mammalian tissue engineered myocardium has, however, puzzled the field for almost 20 years. By combining mechanical and electrical stimulation to enable auxotonic contraction at a developmental stage-adapted beating frequency (4 Hz (19)), we succeeded in achieving this missing physiological property in tissue engineered myocardium. Notably, the positive FFR was not developed by entraining EHM under mechanical loading at sub-physiological beating frequencies (2 Hz) or by mechanical loading alone. Enhanced functional maturation - evidenced by the positive FFR, FDAR, and a right-shifted calcium response curve, was paralleled by enhanced T-tubulation and maturation of SR calcium handling, providing a mechanistic underpinning for the observed functional phenotype (Figure 6E).

Despite obvious and surprisingly similar advances in maturation in mechanically (9, 10, 14, 24, 25) and electrically (12, 13, 20, 26) stimulated engineered myocardium, there has been no successful attempt to control beating rate of engineered myocardium during extended tissue culture at physiological beating frequencies. In fact, sustained electrical stimulation at higher frequencies is technically challenging and may be confounded by bystander effects (i.e., electrolysis, pH-shift, generation of reactive oxygen species) (27). By adapting a previously developed electrical stimulation protocol (13, 28) to EHM culture (14) we could overcome these limitations and robustly capture EHM at 2 Hz and the physiological neonatal rate of 4 Hz for at least 5 days without apparent “electro-toxicity”. EHM could not be captured reliably at supra-physiological beating rates (6 Hz) and it will require additional refinements of our electro-mechanical stimulation protocol to simulate the physiological increase in beating frequency during postnatal heart development (19) in EHM cultures *in vitro*.

The positive FFR (first described by Bowditch in 1871) has been confirmed in ventricular myocardium of nearly all classical experimental animal models and humans (1). It develops postnatally as a fundamental property of the mature heart (29) and is typically lost in heart failure (30). For rat, a biphasic FFR has been described with a negative slope at unphysiologically low beating frequencies (0.05–1 Hz) and a positive slope at physiological beating frequencies (2–4 Hz (19)). Our findings suggest that the development of the positive FFR - in contrast to other classical physiological properties of heart muscle such as Frank-Starling mechanism and inotropic responsiveness to catecholamines - appears to be strictly dependent on beating frequency and concomitant maturation of intracellular calcium handling. Advanced maturation of calcium handling in EHM was also evidenced by a right-shift in calcium EC_{50} (0.45 to 0.7 mmol/L; $P < 0.05$) and accelerated intracellular calcium release and uptake kinetics. These findings closely resemble observations from postnatal rat hearts, but also suggest that further optimization of the reported electro-mechanical stimulation protocol - for example by dynamic adaptation of electrical stimulation according to observed changes during postnatal development, prolongation of culture, or addition of growth supplements - may be necessary to advance maturation towards an adult stage.

The observed molecular changes in EHM (enhanced SERCA2a protein abundance; enhanced susceptibility to pharmacological RyR2 blockade) are consistent with the observed acceleration of intracellular calcium release and decay as well as with the enhanced post-rest potentiation. In line with its fundamental importance for the Bowditch phenomenon, high SERCA2a protein expression was associated with a positive FFR and low SERCA2a with a negative FFR (31). These observations form the rationale for ongoing clinical trials, aiming at SERCA normalization in heart failure (32).

A particularly interesting observation was the establishment of regular striated, apparently mature RyR2 organization despite limited T-tubulation, which is in line with previous observation (11, 33). It is well known that the T-tubule associated calcium handling machinery matures only postnatally, which involves nanometric approximation of LTCCs (Cav1.2) located mainly in T-tubule membranes to RyR2 channels in jSR domain (34). In rat, T-tubules first develop around postnatal day 10, and achieve near-adult differentiation by postnatal day 20 (5, 35). Initial stages of T-tubule development depend on vesicles and

longitudinal T-tubule elements in skeletal and heart muscles (36–38); internal jSR associations with transverse T-tubules are found later in fully mature muscle (39–41). The latter process may in fact not be required for optimal calcium provision in the smaller early postnatal cardiomyocytes, but seems essential to accommodate the then rapidly occurring hypertrophic growth. This finding is also supported by the increase in perpendicular T-tubules in cardiomyocyte from 13 day old rats which were clearly larger as compared to cardiomyocytes from EHM (940 vs. 560 μm^2).

We conclude that electro-mechanical stimulation at physiological frequency is necessary to achieve a positive FFR through the maturation of ventricular cardiomyocytes. Integration of electro-mechanical control algorithms into myocardial tissue engineering appear especially important if a mismatch between *in vivo* and *in vitro* beating rate is observed. The rat EHM model was particularly well suited to address the fundamental role for frequency control in cardiomyocyte maturation, as it exhibits a sub-physiological spontaneous beating rate (this is in contrast to human EHM with an endogenous beating frequency of 0.5–1.5 Hz (25)). The rat system is also well positioned to answer questions about SR maturation and t-tubular development as concordant with functional maturation, as these processes occur postnatally. At this time, there is little evidence that human engineered myocardium derived from from embryonic or induced pluripotent stem cells can reach a phenotypically postnatal stage. Better control of maturation in tissue engineered myocardium is undoubtedly important to advance its utility as a tool in cardiovascular research. To this end, benchmarking key physiological determinants of mature and healthy myocardium is of fundamental importance. The observation that a classical Bowditch phenomenon can be engineered *in vitro* by maintaining a physiological beating frequency adds a new paradigm to current tissue engineering approaches and further confirms that the Bowditch phenomenon is intricately connected to maturation of ventricular cardiomyocytes.

4. Methods

4.1 EHM construction and culture

EHMs were made from mixtures of collagen type I, Matrigel™ and neonatal rat heart cells (2.5×10^6) as previously described (14). EHM culture medium was supplemented with Insulin-Transferrin-Selenium-X (Gibco Life Technologies) during culture days 1–7 (42). EHMs were cast into circular molds and allowed to condense for 1 week (Figure 1A–B) (9). On culture day 7, EHMs were transferred onto stretchers to support auxotonic contractions (Figure 1C) (14). From culture day 8, EHMs were cultured for an additional 5 days with or without electrical stimulation (2, 4, or 6 Hz; 3 ms biphasic 5 V pulses; Suppl. Movie) using the C-dish and C-Pace EP Culture Pacer (Ionoptix, Figure 1D). EHM had a cross sectional area 1.51 ± 0.06 mm^2 (n=15) without differences between investigated groups.

4.2 Isometric Force Measurements

On culture day 13, EHMs were transferred to organ baths containing oxygenated Tyrode's solution at 37°C for isometric force measurements (10). Spontaneous beating rates of EHMs were recorded. EHMs were then preloaded at 2 Hz electrical field stimulation (200 mA, 5 ms) by stepwise length adjustment, until the length for maximum force generation (Lmax)

according to the Frank-Starling mechanism was reached. Maximal inotropic capacity was measured under cumulatively increasing extracellular calcium (0.2 – 2.8 mmol/L). Ryanodine (1 μmol/L, Calbiochem) was added to block systolic SR-calcium release. SR-calcium loading was further analyzed by post-rest potentiation (PRP) measurements (43). For PRP measurements, EHMs were paced for 3 minutes until contractile stability was achieved. The amplitude (i.e., twitch force) of the first beat after stimulation pauses of 10, 20, or 30 seconds (2 minutes apart) was recorded and related to the last beat before the stimulation pause. EHMs with spontaneous contractions during the pauses were excluded from analysis.

4.3 Cardiomyocyte Isolation from EHMs

EHMs were immersed in a buffer containing 113 mmol/L NaCl, 4.7 mmol/L KCl, 0.6 mmol/L KH_2PO_4, 0.6 mmol/L $Na_2HPO_4 \times 2H_2O$, 1.2 mmol/L $MgSO_4 \times 7H_2O$, 12 mmol/L $NaHCO_3$, 10 mmol/L $KHCO_3$, 10 mmol/L HEPES, 30 mmol/L Taurine, supplemented with Liberase Blendzyme TM (Roche) and 30 mmol/L 2,3-butaneodione monoxime (BDM) at 37°C for 1 hour. Enzyme activity was quenched with bovine serum albumin and calcium concentration was readjusted step-wise to 1 mmol/L. Isolated single cells were plated onto laminin-coated (10 μg/ml) cover slips for calcium imaging. Cardiomyocytes from 13 day-old rats were isolated using a modified Langendorff method as described previously (44).

4.4 Calcium Imaging

Single cells isolated from EHMs were loaded with Fura-2 dye (1 μmol/L) for 20 minutes, washed with the cell isolation buffer (without enzyme and BDM). Cells were imaged using the Myocyte Calcium and Contractility Recording System (IonOptix). Transients were recorded at room temperature under 1 Hz stimulation and analyzed using IonWizard software (IonOptix). Cardiomyocytes were additionally treated with a rapid administration of caffeine (10 mmol/L, Calbiochem) or thapsigargin (45) (1 μmol/L, Calbiochem) for 3 minutes, to assess SR storage capacity and dependence on SERCA-mediated Ca^{2+} re-uptake from the cytosol, respectively.

4.5 Immunoblotting

EHMs were washed thoroughly in ice cold PBS and rapidly homogenized in lysis buffer containing 30 mmol/L Tris (pH 8.8), 5 mmol/L EDTA (pH 8), 3% SDS, 10% glycerol, 30 mmol/L NaF, and phosphatase inhibitors (Roche Applied Science). After centrifugation at 12,000 g for 10 min, supernatants containing soluble proteins were resolved by SDS-PAGE and transferred onto nitrocellulose membranes. Primary antibodies used were: CSQ2 (1:2.500; ABR-01164 Dianova), GAPDH (1:50.000; RGM2-6CS Zytomed Systems), RyR2 (1:1.000; HPA020028 Sigma Aldrich Prestige), SERCA2a (1:200; sc-8094 Santa Cruz Biotech), LTCC (1:250; sc-81890 Santa Cruz). Primary antibodies were detected with appropriate horseradish peroxidase coupled secondary antibodies. Chemiluminescence signals were enhanced with the LumiLight Western Blotting Substrate (Roche) or SuperSignal West Dura Chemiluminescent Substrate (Thermo Scientific), detected with the Molecular Imager VersaDoc MP 4000 System (Bio-Rad), and quantified using QuantityOne software (Bio-Rad).

4.6 Flow Cytometry and Cell Viability

Cells isolated from day 13 EHMs were incubated with 40 μg/mL wheat germ agglutinin (WGA; Alexa Fluor 555 Conjugate, Life Technologies) for 15 minutes at 37°C, and subsequently fixed in 4% formaldehyde. Cells were then incubated with a primary antibody against α-actinin (Sigma) followed by a secondary antibody (Alexa Fluor 488 anti-mouse IgG). Samples were labeled with DAPI (1 μg/ml) and flow cytometry was performed on an LSRII (BD Biosciences). Flow cytometry results were analyzed using FacsDiva software (BD Biosciences) or Cyflogic software. Negative controls were stained only with secondary antibody and DAPI. The gating strategy used DAPI to exclude cell fragments and multicellular clumps as well as α-actinin to distinguish cardiomyocytes from non-myocytes (Figure S2). Cell number and viability were measured with the electrical current exclusion method using the CASY TT system (Roche).

4.7 T-tubule Imaging and Analysis

Single cardiomyocytes were obtained from day 13 EHMs or day 13 rats as described above. Isolated cardiomyocytes were immediately labeled with 50 μmol/L di-8-ANEPPS (Life Technologies) for 15 min at room temperature. Membranes were imaged using a confocal laser scanning microscope (Zeiss, LSM 710), a 63x 1.4 NA oil objective, excitation at 458 nm, and a detection range between 550 nm and 740 nm. T-tubule networks were analyzed as described previously using Fiji (36). Briefly, after background subtraction, local contrast enhancement, smoothing and statistical region merging, images were binarized and skeletons were extracted applying the plugin “Skeletonize (2D/3D)” (Figure S3). T-tubule network properties were obtained applying “Analyze Skeleton (2D/3D)”. T-tubule density was measured as the total skeleton length normalized to the area.

4.8 Statistical analyses

Experimental data are presented as mean ± S.E.M. Data were analyzed using appropriate statistical tests as indicated using GraphPad Prism software. $P < 0.05$ was considered significant.

4.9 Study approval

Harvest of hearts from neonatal rats was approved by the Niedersächsisches Landesamt für Verbraucherschutz und Lebensmittelsicherheit (LAVES).

Supplementary Material

Refer to Web version on PubMed Central for supplementary material.

Acknowledgments

We acknowledge the excellent assistance of A. Schraut and K. Schenk with cardiomyocyte preparations.

Sources of Funding

The authors are supported by the DZHK (German Center for Cardiovascular Research to W.H.Z. and S.E.L.), the German Federal Ministry for Science and Education (BMBF FKZ 13GW0007A [CIRM]) to W.H.Z., the German Research Foundation (DFG ZI 708/7-1, 8-1, 10-1, SFB 1002 TP A05 and C04 and TP S – to W.H.Z., A.E.A, and

S.E.L.), the European Union FP7 CARE-MI to W.H.Z, and the NIH (U01 HL099997 to W.H.Z.; R01 HL076485 and P41 EB002520 to G.V.N.).

Appendix A. Supplementary data

Supplementary data related to this article can be found at http://dx.doi.org/10.1016/j.biomaterials.2015.03.055

References

1. Endoh M. Force-frequency relationship in intact mammalian ventricular myocardium: physiological and pathophysiological relevance. European journal of pharmacology. 2004; 500(1–3):73–86. [PubMed: 15464022]
2. Bers, DM. Excitation-Contraction Coupling and Cardiac Contractile Force. Dordrecht, Netherlands: Kluwer Academic; 2001.
3. Katz, AM. Heart Failure Pathophysiology, Molecular Biology, and Clinical Management. Philadelphia, USA: Lippcott Williams & Wilkins; 2000.
4. Olivetti G, Anversa P, Loud AV. Morphometric study of early postnatal development in the left and right ventricular myocardium of the rat. II. Tissue composition, capillary growth, and sarcoplasmic alterations. Circulation research. 1980; 46(4):503–12. [PubMed: 6444555]
5. Ziman AP, Gomez-Viquez NL, Bloch RJ, Lederer WJ. Excitation-contraction coupling changes during postnatal cardiac development. Journal of molecular and cellular cardiology. 2010; 48(2): 379–86. [PubMed: 19818794]
6. Bers DM. Cardiac excitation-contraction coupling. Nature. 2002; 415(6868):198–205. [PubMed: 11805843]
7. Tiburcy M, Zimmermann WH. Modeling myocardial growth and hypertrophy in engineered heart muscle. Trends Cardiovasc Med. 2014; 24(1):7–13. [PubMed: 23953977]
8. Eschenhagen T, Eder A, Vollert I, Hansen A. Physiological aspects of cardiac tissue engineering. American journal of physiology Heart and circulatory physiology. 2012; 303(2):H133–43. [PubMed: 22582087]
9. Tiburcy M, Didie M, Boy O, Christalla P, Doker S, Naito H, Karikkineth BC, El-Armouche A, Grimm M, Nose M, et al. Terminal differentiation, advanced organotypic maturation, and modeling of hypertrophic growth in engineered heart tissue. Circulation research. 2011; 109(10):1105–14. [PubMed: 21921264]
10. Zimmermann WH, Fink C, Kralisch D, Remmers U, Weil J, Eschenhagen T. Three-dimensional engineered heart tissue from neonatal rat cardiac myocytes. Biotechnol Bioeng. 2000; 68(1):106–14. [PubMed: 10699878]
11. Zimmermann WH, Schneiderbanger K, Schubert P, Didie M, Munzel F, Heubach JF, Kostin S, Neuhuber WL, Eschenhagen T. Tissue engineering of a differentiated cardiac muscle construct. Circulation research. 2002; 90(2):223–30. [PubMed: 11834716]
12. Radisic M, Park H, Shing H, Consi T, Schoen FJ, Langer R, Freed LE, Vunjak-Novakovic G. Functional assembly of engineered myocardium by electrical stimulation of cardiac myocytes cultured on scaffolds. Proc Natl Acad Sci U S A. 2004; 101(52):18129–34. [PubMed: 15604141]
13. Tandon N, Cannizzaro C, Chao PH, Maidhof R, Marsano A, Au HT, Radisic M, Vunjak-Novakovic G. Electrical stimulation systems for cardiac tissue engineering. Nat Protoc. 2009; 4(2):155–73. [PubMed: 19180087]
14. Zimmermann WH, Melnychenko I, Wasmeier G, Didie M, Naito H, Nixdorff U, Hess A, Budinsky L, Brune K, Michaelis B, et al. Engineered heart tissue grafts improve systolic and diastolic function in infarcted rat hearts. Nat Med. 2006; 12(4):452–8. [PubMed: 16582915]
15. Zimmermann WH. Biomechanical regulation of in vitro cardiogenesis for tissue-engineered heart repair. Stem cell research & therapy. 2013; 4(6):137. [PubMed: 24229468]
16. Berger HJ, Prasad SK, Davidoff AJ, Pimental D, Ellingsen O, Marsh JD, Smith TW, Kelly RA. Continual electric field stimulation preserves contractile function of adult ventricular myocytes in primary culture. Am J Physiol. 1994; 266(1 Pt 2):H341–9. [PubMed: 8304516]

17. Holt E, Lunde PK, Sejersted OM, Christensen G. Electrical stimulation of adult rat cardiomyocytes in culture improves contractile properties and is associated with altered calcium handling. Basic Res Cardiol. 1997; 92(5):289–98. [PubMed: 9486350]

18. Ivester CT, Kent RL, Tagawa H, Tsutsui H, Imamura T, Cooper Gt, McDermott PJ. Electrically stimulated contraction accelerates protein synthesis rates in adult feline cardiocytes. Am J Physiol. 1993; 265(2 Pt 2):H666–74. [PubMed: 8368369]

19. Vornanen M. Force-frequency relationship, contraction duration and recirculating fraction of calcium in postnatally developing rat heart ventricles: correlation with heart rate. Acta physiologica Scandinavica. 1992; 145(4):311–21. [PubMed: 1529721]

20. Lasher RA, Pahnke AQ, Johnson JM, Sachse FB, Hitchcock RW. Electrical stimulation directs engineered cardiac tissue to an age-matched native phenotype. Journal of tissue engineering. 2012; 3(1):2041731412455354. [PubMed: 22919458]

21. Bers DM. Ca influx and sarcoplasmic reticulum Ca release in cardiac muscle activation during postrest recovery. Am J Physiol. 1985; 248(3 Pt 2):H366–81. [PubMed: 2579587]

22. Koch-Weser J, Blinks JR. The Influence of the Interval between Beats on Myocardial Contractility. Pharmacol Rev. 1963; 15:601–52. [PubMed: 14064358]

23. Kort AA, Lakatta EG. Spontaneous sarcoplasmic reticulum calcium release in rat and rabbit cardiac muscle: relation to transient and rested-state twitch tension. Circulation research. 1988; 63(5):969–79. [PubMed: 3180359]

24. Tulloch NL, Muskheli V, Razumova MV, Korte FS, Regnier M, Hauch KD, Pabon L, Reinecke H, Murry CE. Growth of engineered human myocardium with mechanical loading and vascular coculture. Circulation research. 2011; 109(1):47–59. [PubMed: 21597009]

25. Soong PL, Tiburcy M, Zimmermann WH. Cardiac differentiation of human embryonic stem cells and their assembly into engineered heart muscle. Current protocols in cell biology / editorial board, Juan S Bonifacino [et al]. 2012 Chapter 23(Unit23 8.

26. Nunes SS, Miklas JW, Liu J, Aschar-Sobbi R, Xiao Y, Zhang B, Jiang J, Masse S, Gagliardi M, Hsieh A, et al. Biowire: a platform for maturation of human pluripotent stem cell-derived cardiomyocytes. Nature methods. 2013; 10(8):781–7. [PubMed: 23793239]

27. Hirt MN, Boeddinghaus J, Mitchell A, Schaaf S, Bornchen C, Muller C, Schulz H, Hubner N, Stenzig J, Stoehr A, et al. Functional improvement and maturation of rat and human engineered heart tissue by chronic electrical stimulation. Journal of molecular and cellular cardiology. 2014(74C):151–61. [PubMed: 24852842]

28. Tandon N, Marsano A, Maidhof R, Wan L, Park H, Vunjak-Novakovic G. Optimization of electrical stimulation parameters for cardiac tissue engineering. J Tissue Eng Regen Med. 2011; 5(6):e115–25. [PubMed: 21604379]

29. Wiegerinck RF, Cojoc A, Zeidenweber CM, Ding G, Shen M, Joyner RW, Fernandez JD, Kanter KR, Kirshbom PM, Kogon BE, et al. Force frequency relationship of the human ventricle increases during early postnatal development. Pediatric research. 2009; 65(4):414–9. [PubMed: 19127223]

30. Mulieri LA, Hasenfuss G, Leavitt B, Allen PD, Alpert NR. Altered myocardial force-frequency relation in human heart failure. Circulation. 1992; 85(5):1743–50. [PubMed: 1572031]

31. Hasenfuss G, Mulieri LA, Leavitt BJ, Alpert NR. Influence of isoproterenol on contractile protein function, excitation-contraction coupling, and energy turnover of isolated nonfailing human myocardium. Journal of molecular and cellular cardiology. 1994; 26(11):1461–9. [PubMed: 7897670]

32. Greenberg B, Yaroshinsky A, Zsebo KM, Butler J, Felker GM, Voors AA, Rudy JJ, Wagner K, Hajjar RJ. Design of a phase 2b trial of intracoronary administration of AAV1/SERCA2a in patients with advanced heart failure: the CUPID 2 trial (calcium up-regulation by percutaneous administration of gene therapy in cardiac disease phase 2b). JACC Heart failure. 2014; 2(1):84–92. [PubMed: 24622121]

33. Bian W, Badie N, Himel HDt, Bursac N. Robust T-tubulation and maturation of cardiomyocytes using tissue-engineered epicardial mimetics. Biomaterials. 2014; 35(12):3819–28. [PubMed: 24508078]

34. Scriven DRL, Asghari P, Schulson MN, Moore EDW. Analysis of Cav1.2 and ryanodine receptor clusters in rat ventricular myocytes. Biophys J. 2010; 99(12):3923–9. [PubMed: 21156134]

35. Reynolds JO, Chiang DY, Wang W, Beavers DL, Dixit SS, Skapura DG, Landstrom AP, Song LS, Ackerman MJ, Wehrens XH. Junctophilin-2 is necessary for T-tubule maturation during mouse heart development. Cardiovascular research. 2013; 100(1):44–53. [PubMed: 23715556]

36. Wagner E, Lauterbach MA, Kohl T, Westphal V, Williams GSB, Steinbrecher JH, Streich JH, Korff B, Tuan HTM, Hagen B, et al. Stimulated Emission Depletion Live-Cell Super-Resolution Imaging Shows Proliferative Remodeling of T-Tubule Membrane Structures After Myocardial Infarction. Circulation research. 2012; 111(4):402–14. [PubMed: 22723297]

37. Sperelakis N, Rubio R. An orderly lattice of axial tubules which interconnect adjacent transverse tubules in guinea-pig ventricular myocardium. Journal of molecular and cellular cardiology. 1971; 2(3):211–20. [PubMed: 5117216]

38. Soeller C, Cannell MB. Examination of the transverse tubular system in living cardiac rat myocytes by 2-photon microscopy and digital image-processing techniques. Circulation research. 1999; 84(3):266–75. [PubMed: 10024300]

39. Parton RG, Way M, Zorzi N, Stang E. Caveolin-3 associates with developing T-tubules during muscle differentiation. The Journal of Cell Biology. 1997; 136(1):137–54. [PubMed: 9008709]

40. Takekura H, Flucher BE, Franzini-Armstrong C. Sequential docking, molecular differentiation, and positioning of T-Tubule/SR junctions in developing mouse skeletal muscle. Developmental biology. 2001; 239(2):204–14. [PubMed: 11784029]

41. Franzini-Armstrong C. Veratti and Beyond: Structural Contributions to the Study of Muscle Activation. Rend Fis Acc Lincei. 2002; 13(9):289–323.

42. Naito H, Melnychenko I, Didie M, Schneiderbanger K, Schubert P, Rosenkranz S, Eschenhagen T, Zimmermann WH. Optimizing engineered heart tissue for therapeutic applications as surrogate heart muscle. Circulation. 2006; 114(1 Suppl):I72–8. [PubMed: 16820649]

43. Schouten VJ, van Deen JK, de Tombe P, Verveen AA. Force-interval relationship in heart muscle of mammals. A calcium compartment model. Biophys J. 1987; 51(1):13–26. [PubMed: 3801581]

44. Gotz KR, Nikolaev VO. Advances and techniques to measure cGMP in intact cardiomyocytes. Methods in molecular biology. 2013(1020):121–9. [PubMed: 23709029]

45. Schwoerer AP, Neef S, Broichhausen I, Jacubeit J, Tiburcy M, Wagner M, Biermann D, Didie M, Vettel C, Maier LS, et al. Enhanced Ca(2)+ influx through cardiac L-type Ca(2)+ channels maintains the systolic Ca(2)+ transient in early cardiac atrophy induced by mechanical unloading. Pflugers Arch. 2013; 465(12):1763–73. [PubMed: 23842739]

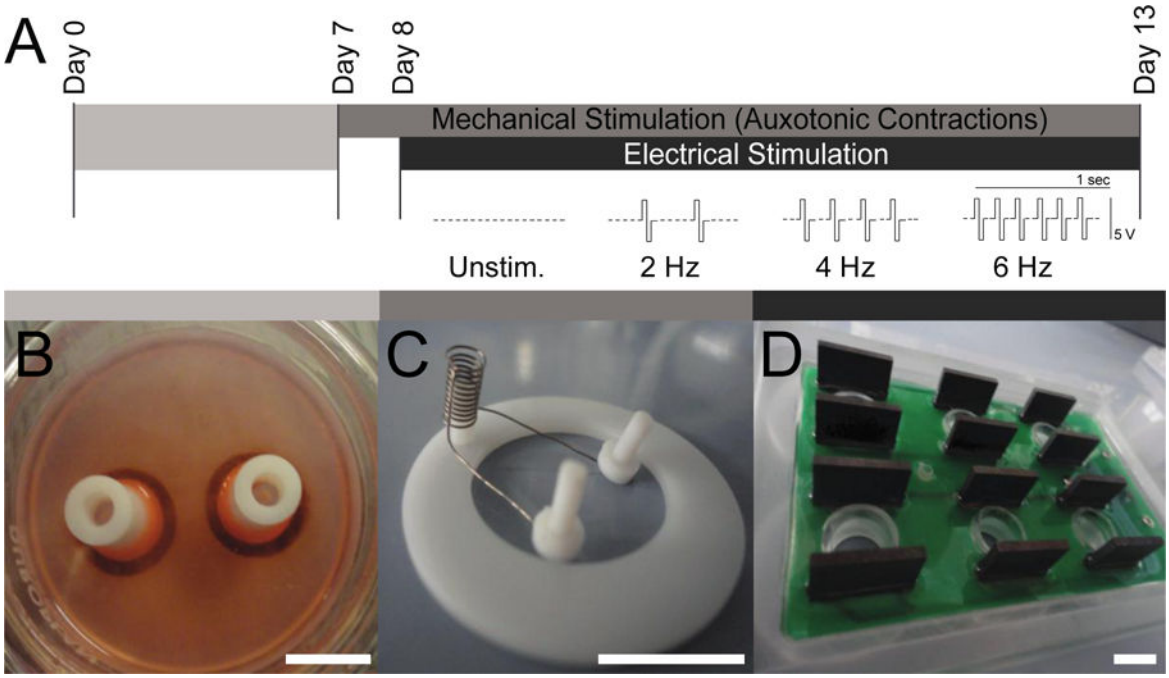

Figure 1. Experimental Design

A. EHMs were cultured over a 13-day period, with an 8-day consolidation phase (7 days in casting mold [**B**] plus 1 day on DMS [**C**]) followed by a 5 day maturation phase under electro-mechanical stimulation (DMS plus 3 ms biphasic 5 V pulses at 2, 4, or 6 Hz); unstimulated, i.e. spontaneously and auxotonically beating EHMs (Unstim.) served as controls. **B.** Casting mold with two already condensed EHMs. **C.** Custom made stretch device for DMS to support auxotonic contractions of EHMs. **D.** C-dish stimulation plate (Ionoptix) used to deliver square biphasic pulses to EHMs via graphite electrodes. Scale bars: 10 mm.

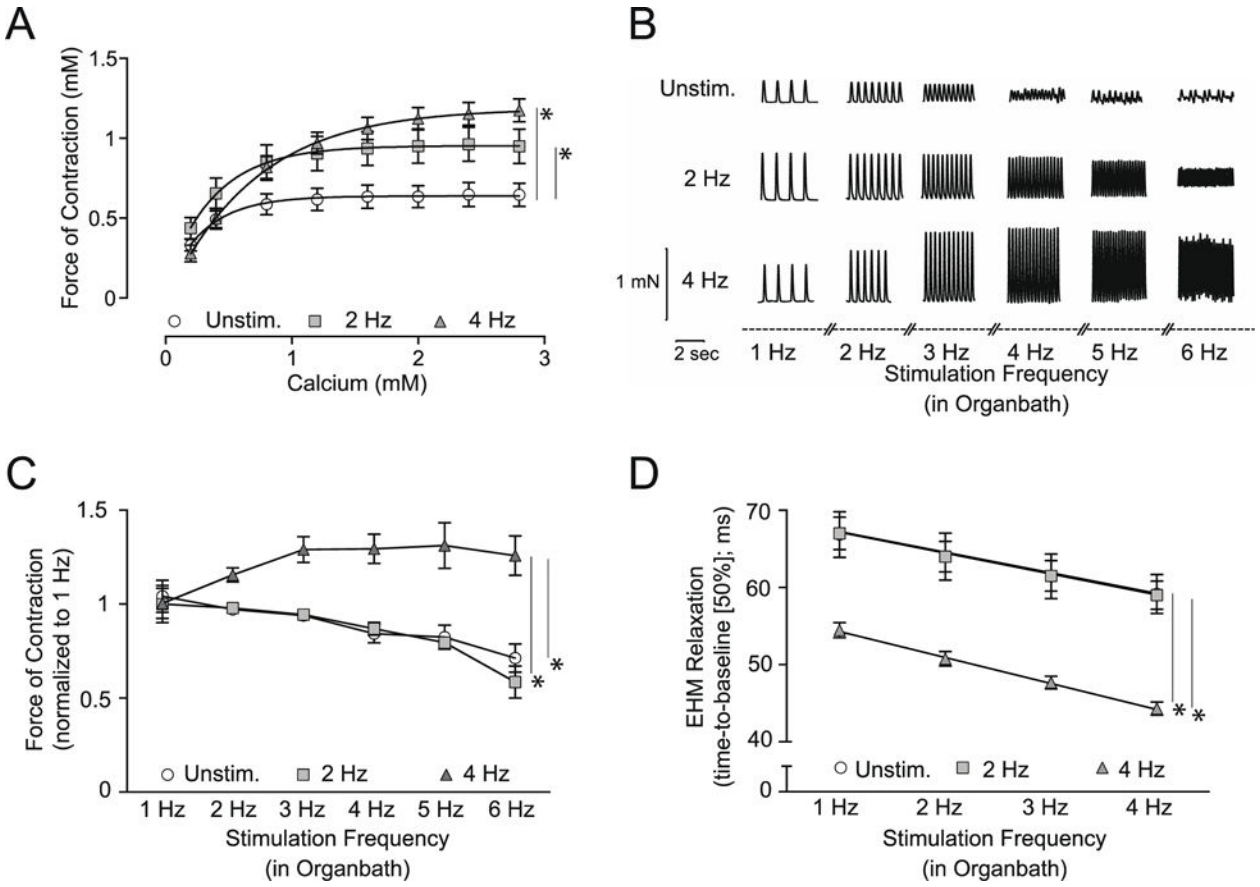

Figure 2. Maturation of Contractile Parameters and Force-Frequency Relationship by Electro-Mechanical Stimulation

A. Concentration response curve for extracellular calcium (0.2 to 2.8 mmol/L) to assess the maximal inotropic capacity of EHM; n=16/11/16 (EHMs per group); $*P < 0.05$ vs. Unstim. by repeated measures ANOVA followed by Bonferroni's multiple comparison test. **B.** Representative contraction amplitudes of EHM recorded at the indicated stimulation frequencies (1–6 Hz field stimulation in organ bath) on culture day 13. **C**. Summary of isometric force of contraction data measured at increasing stimulation frequencies (1–6 Hz); note the positive FFR (Bowditch phenomenon) only in EHM electro-mechanically conditioned during culture at 4 Hz; n=15/8/13 (EHM per group); force of contraction (FOC) normalized to baseline FOC at 1 Hz stimulation; *P < 0.05 vs. Unstim. and 2 Hz by repeated measures ANOVA followed by Bonferroni's multiple comparison test. **D**. Evaluation of relaxation time (time-to-baseline [50%]) and frequency-dependent acceleration of relaxation (FDAR – slope of linear regression is significantly steeper in 4 Hz vs. 2 Hz and Unstim. EHM, P<0.05) in EHM developed under electro-mechanical stimulation vs. Unstim.-EHM at 1, 2, 3, and 4 Hz field stimulation; n=14/8/13 (EHM per group); *P < 0.05 vs. Unstim. and 2 Hz by repeated ANOVA followed by Bonferroni's multiple comparison test.

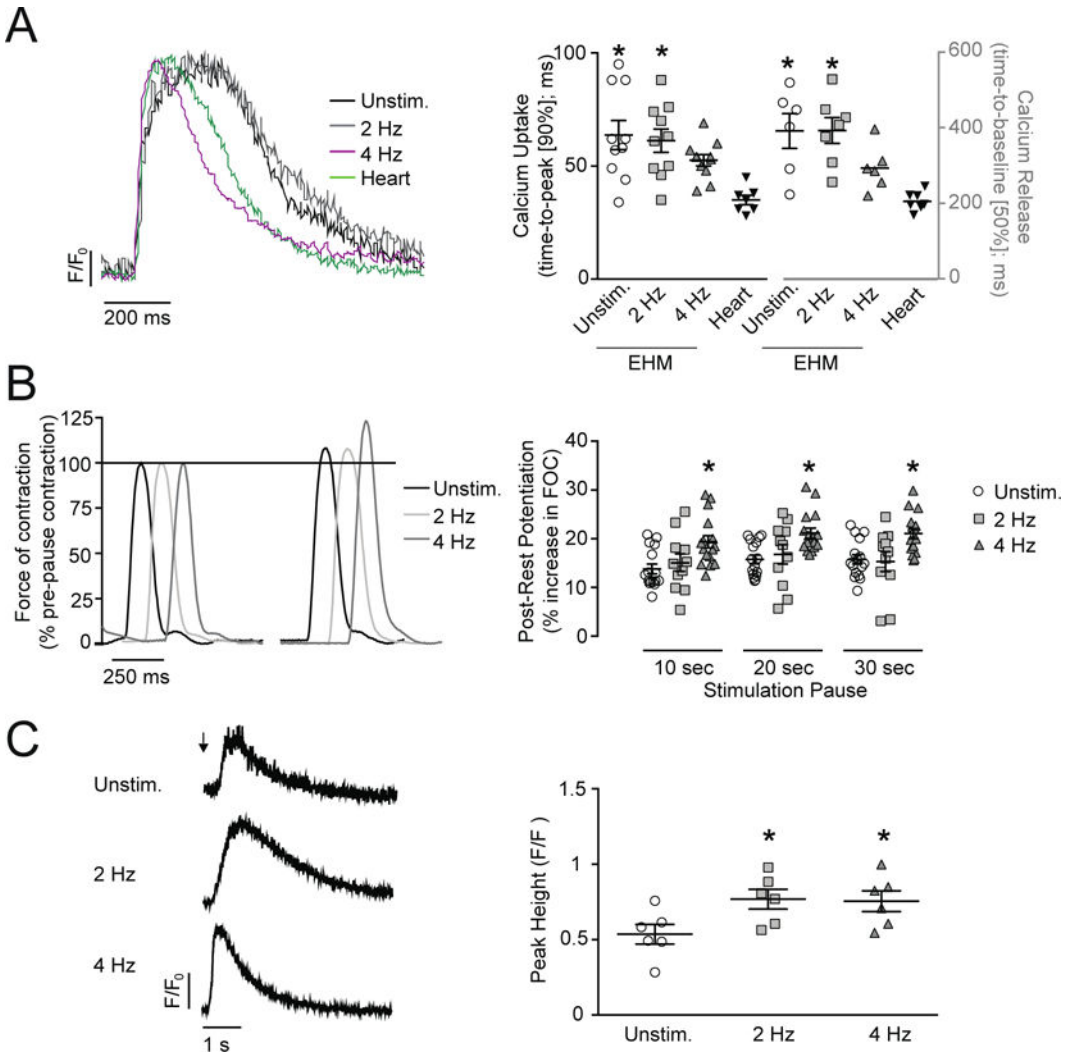

Figure 3. Maturation of Calcium Handling in EHM-derived Cardiomyocytes

A. Representative calcium transients from EHM-derived and 13-day old rat heart-derived cardiomyocytes recorded at 1 Hz field-stimulation after loading with fura-2; F/F_0: change of fluorescent signal over background fluorescence. x/y-graphs: time-to-peak; n=10/10/11/7 cardiomyocytes (90%; calcium release) and time-to-baseline; n=6/7/6/7 cardiomyocytes (50%; calcium decay) fura-2 signal. **B.** Representative traces before and after a 30 s stimulation pause. Force of contraction (FOC) was normalized to pre-pause baseline values at 2 Hz field stimulation. x/y-graph: FOC increase of the first post-rest twitch after 10, 20, 30 second rest; n=16/11/16 (EHM per group). **C.** Original recordings of fura-2 signals from unstimulated EHM-derived cardiomyocytes after exposure to a caffeine puff (10 mmol/L; arrow). x/y-graph: maximal peak height of fura-2 signal (F/F_0) after caffeine-induced calcium release; n=6/6/6 cardiomyocytes. *$P < 0.05$ vs. 13-day old rat heart-derived cardiomyocytes (Heart; **A**) or Unstim. (**B, C**) by one-way ANOVA with Bonferroni multiple comparison test (scatter plots with mean ± SEM; symbols in x/y-graphs represent measures from individual EHM- or heart-derived cardiomyocyte (**A, C**) or individual EHMs (**B**).

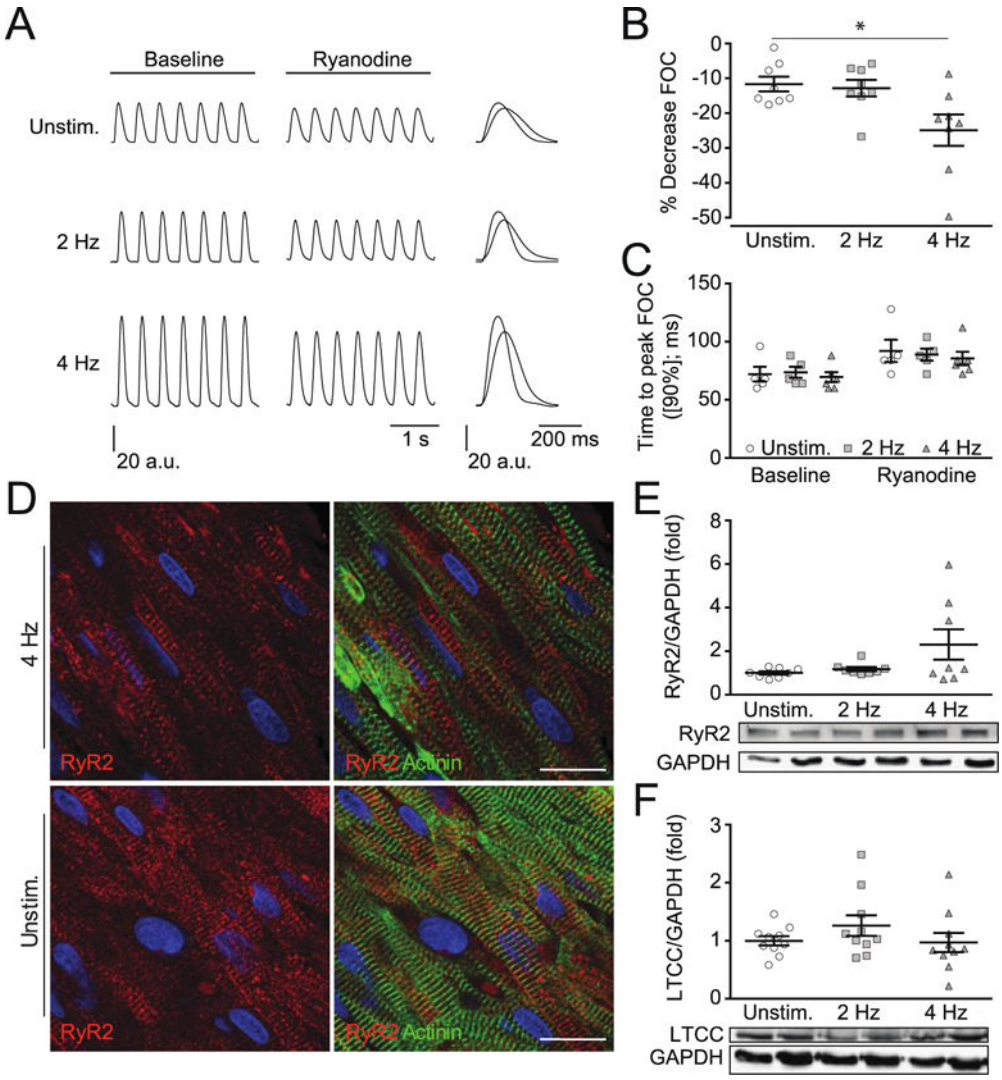

Figure 4. Enhanced RyR2 mediated SR calcium release

A. Representative force traces recorded by isometric contraction measurements in day 13 EHMs before and after Ryanodine treatment (2 min). **B.** Percent decrease in EHM twitch tension at steady-state (under Ryanodine treatment); n=8/8/8 (EHM per group). **C.** contraction time under Ryanodine treatment compared to baseline values; n=5/5/6 (EHM per group). **D.** Representative staining for RyR2 (green) and α-actinin (red) in Unstim. and 4 Hz stimulated EHMs (scale bar: 20 μm). **E.** Western blots and quantification of Ryanodine receptor 2 (RyR2); n=8/8/8 (EHM per group). **F**. L-type Calcium Channel (LTCC); n=10/10/10 (EHM per group). * $P < 0.05$ vs. Unstim. by ANOVA with Bonferroni multiple comparison test (scatter plots with mean ± SEM; symbols represent measures from individual EHMs).

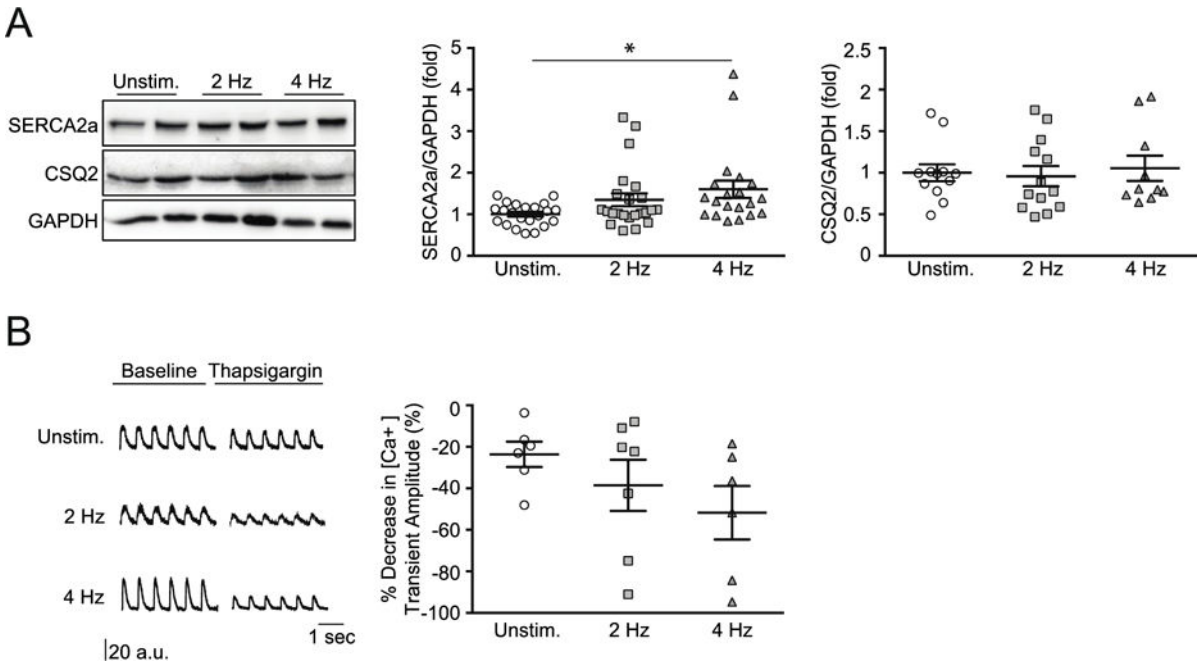

Figure 5. Enhanced SERCA2a mediated SR calcium reuptake

A. Western blot analysis and quantification of day 13 EHMs for SERCA2a (n = 22/23/20 EHM per group) and CSQ2 (n= 12/13/10 EHM per group); data were indexed to GAPDH. **B.** Original recordings of fura-2 signals ($\Delta F/F_0$) from EHM-derived cardiomyocytes under field stimulation at 1 Hz before and 2 min after addition of thapsigargin (1 μmol/L); signal quantification demonstrated a trend to a most pronounced thapsigargin effect in the 4 Hz group; n= 6/7/6 cardiomyocytes. * $P < 0.05$ vs. Unstim. by ANOVA with Bonferroni multiple comparison test (scatter plots with mean ± SEM; symbols represent measures from individual EHMs in **A** and EHM-derived cardiomyocytes in **B**).

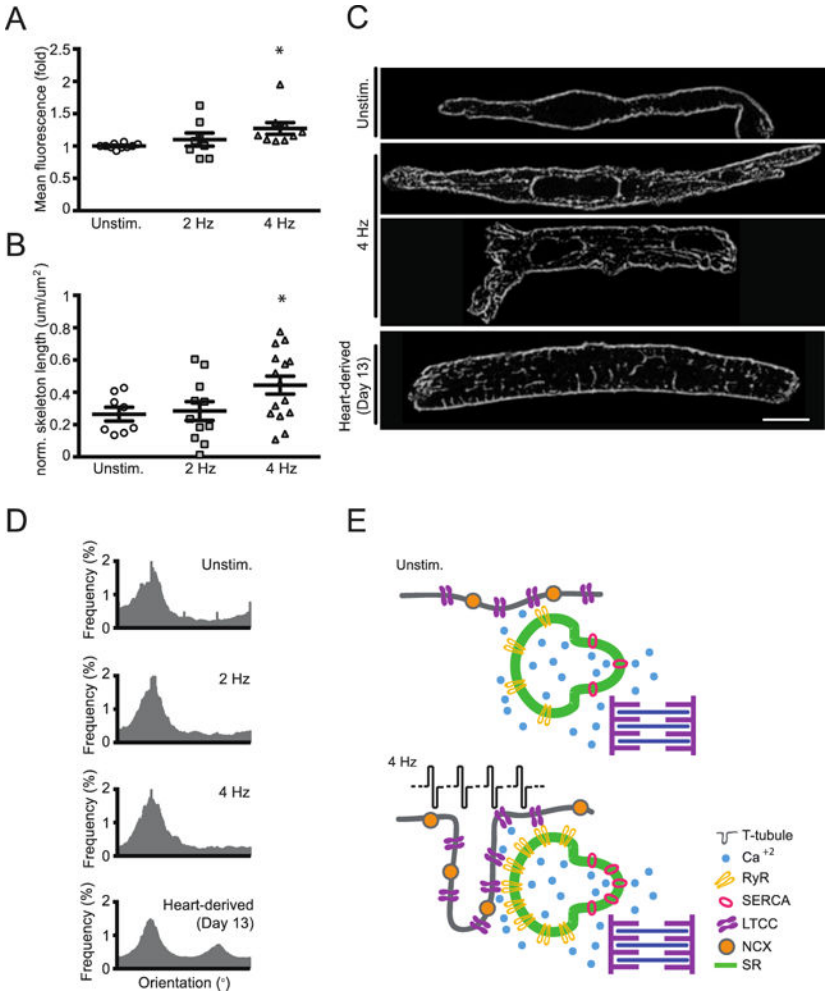

Figure 6. Enhanced T-tubulation under 4 Hz electro-mechanical stimulation

A. Wheat germ agglutinin (WGA) signal intensity, as a correlate for cell surface area, assessed by flow cytometry; mean WGA expression in α-actinin positive cardiomyocytes was evaluated (n=10/9/8 cardiomyocytes); * $P < 0.05$ vs. Unstim. by ANOVA with Bonferroni multiple comparison test (scatter plots with mean ± SEM; symbols represent measures from cardiomyocyte pools derived from individual EHMs). **B**. Quantification of "intracellular" di-8-ANEPPS signal, labelling of *bona fide* t-tubuli, in EHM-derived cardiomyocytes; n=10/9/8 cardiomyocytes, * $P < 0.05$ vs. Unstim. by ANOVA with Bonferroni multiple comparison test (scatter plots with mean ± SEM; symbols represent measures from individual EHM-derived cardiomyocytes). **C.** Representative images of EHM-derived cardiomyocytes and a day 13 heart-derived cardiomyocyte labeled with di-8-ANEPPS; scale bar: 10 μm. **D.** Histograms showing individual orientations of T-tubule network components for Unstim., 2 Hz, and 4 Hz EHM and day 13-heart derived cardiomyocytes. Orientations of the individual t-tubule network components were analyzed by application of the Fiji plugin "Directionality" on skeletonized images. In EHM-derived cardiomyocytes, the majority of T-tubule components was oriented longitudinally (0°) in relation to the major cell axis; transversally (90°) oriented T-tubule components could be distinguished only in day 13 heart-derived cardiomyocytes. **E.** Graphical summary of key

findings: functional maturity of EHM electrically stimulated to match developmental stage adapted beating frequency (4 Hz) is paralleled by maturation of the calcium-handling machinery with enhanced SERCA2a and RyR2 function as well as *bona fide*, mostly longitudinal T-tubulation.